STUDIES ON SURFACE TENSION INFLUENCED CRITICAL GAP IN CANTILEVER MICROSTRUCTURES

L.-J. Yang * **S. Marimuthu**

Department of Mechanical and Electromechanical Engineering
Tamkang University
New Taipei City, Taiwan

ABSTRACT

This note presents an elasto-capillary model of a cantilever subject to capillary stiction during drying process of removing sacrificial layers in MEMS. Similar to the dynamic analysis of the electrostatic pull-in of electrostatic micro actuators, the cantilever beam tends to be pulled down to the substrate due to the nonlinear capillary force with respect to the gap. The critical one-half gap deformation and the corresponding critical wetting area for pulling down a micro cantilever by surface tension are analytically found herein. The instability situation of a generalized critical deformation for power-law surface force with respect to gap is also predicted accordingly. Some prior MEMS works are exemplified to justify this critical one-half gap deformation for capillary stiction.

Keywords: Stiction, Surface tension, Cantilever, Critical gap.

1. INTRODUCTION

The investigation of the capillary phenomenon could be traced back to the early stage of the 19th century [1-3]. The surface tension and its stiction issue in microelectromechanical systems (MEMS) were firstly studied by Mastrangelo *et al*. [4-6]. Some review articles thereafter addressed this issue [7,8]. Using the surface micromachining to deposit the sacrificial and structural layers in sequence, the sacrificial layer is later removed, the structural layer dipped in deionized (DI) water, and subsequently dried to obtain the free-standing microstructures, *e.g.* cantilever beams. As the water above the free-standing cantilever beams evaporates to some extent, the meniscus surface appears. The liquid beneath the cantilever automatically minimizes its surface. So a pull-down force is exerted on the cantilever to induce vertical deformation and this may cause the stiction problem accordingly due to its high surface-to-volume ratio. In addition, the capillary forces due to the growth of liquid bridge is proved to be dominant in adhesive forces measured with an atomic force microscope (AFM) in ambient air with higher relative humidity [9].

Regarding the surface tension calculation of a MEMS system, the surface energy method is usually used. The total surface tension force of the MEMS device can be deduced by differentiating the surface energy of the whole micro system engaged in liquid with respect to the spatial coordinate [7,10]. The alternative force balance method for studying the surface tension in MEMS, *e.g.*, the capillary rise in the wick structures, considered the surface tension not only at the three-phase interfaces but also on the free surface [11].

The prior works in Ref. [7,11,12] have studied and verified the cantilever deformation due to the capillary force in a static manner. However, the capillary stiction acts more like a switch. It scarcely happens with an in-between situation for sticking a cantilever. In other words, the reality of sticking a cantilever is either with almost no deformation or exactly stuck together with its counterpart. For justifying this idea, in this note the authors addressed the stability of cantilever microstructures. Similar to the analysis of electrostatic "pull-in" phenomenon [13,14], there shows at least two forces including capillary attraction and structure restoring force existing for a cantilever. Finally some prior MEMS works demonstrated to exemplify this elasto-capillary model.

2. THEORETICAL FORMULATION

2.1 The Static Analysis of a Wetted Micro Cantilever

Considering the cantilever involved with the surface stiction in Fig. 1(a), the residual liquid under the cantilever is defined as $(x \times y \times h)$, comparable to the vacant gap space $(L \times W \times h)$ of the cantilever. If the bottom plate or substrate remained fixed, a downward force must be applied to the cantilever. This force has been popularly studied in many prior arts [7,10,11] and is denoted as F_{cap}.

* Corresponding author (Ljyang@mail.tku.edu.tw)

DOI : 10.1017/jmech.2015.50
Copyright © 2015 The Society of Theoretical and Applied Mechanics, R.O.C.
https://doi.org/10.1017/jmech.2015.50 Published online by Cambridge University Press

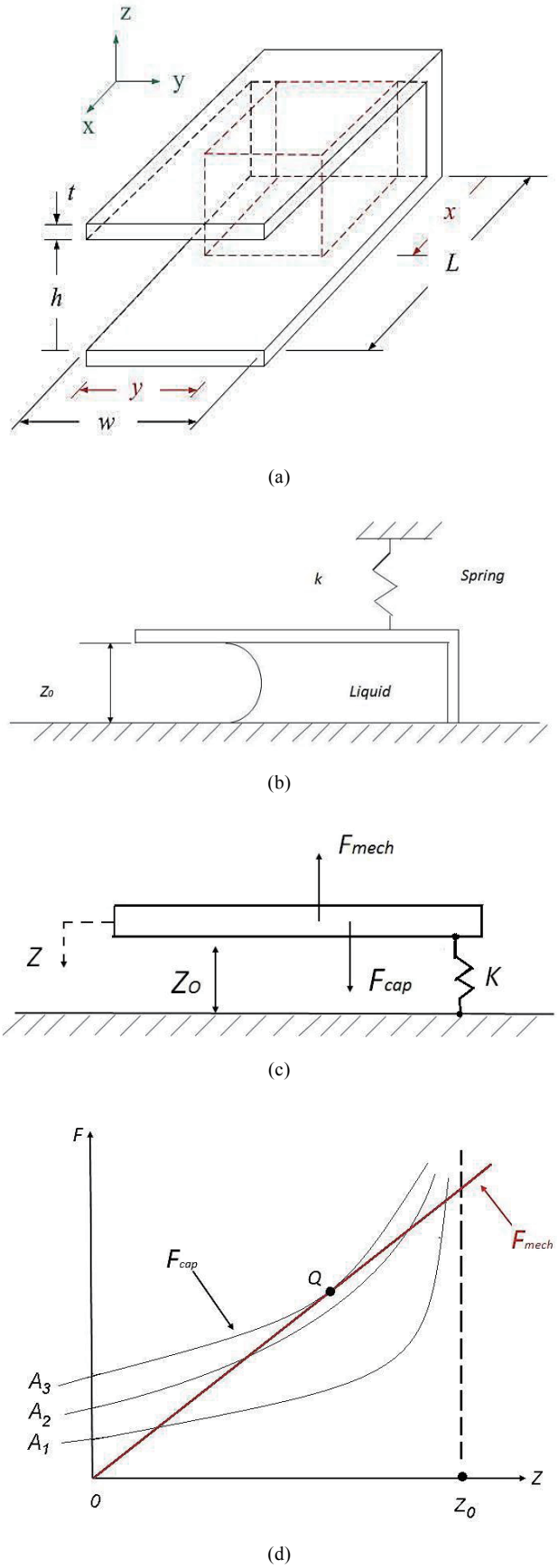


Fig. 1 A micro cantilever: (a) 3D configuration without deflection; (b) the side view with water under the cantilever; (c) capillary force F_{cap} and mechanical restoring force F_{mech}; (d) the force field of F_{mech} and F_{cap}.

$$F_{cap} = -\left(\frac{2A}{h}\right)\gamma_{la}\cos\theta_c \; ; \; A = xy \tag{1}$$

where γ_{la} denotes the liquid-air interfacial surface tension and θ_c denotes the contact angle at the 3-phase interface. Divide Eq. (1) with the solid-liquid surface A and give the capillary pressure or the so-called Laplace pressure exerted on the cantilever.

$$P_{Laplace} = \left|\frac{F_{cap}}{A}\right| = \frac{2\gamma_{la}\cos\theta_c}{h} \tag{2}$$

Equation (2) matches the expression of Laplace pressure mentioned in many prior literatures [2,4-6,7,10,15]. This capillary force increases nonlinearly with the decreasing of the gap h.

On the other hand, a micro cantilever supported by a mechanical spring is in Figs. 1(b) ~ 1(c). The mechanical spring with the force constant k denotes the small deformation behavior of the beam bending. The magnitude of the mechanical restoring force is as below.

$$F_{mech} = kz \tag{3}$$

$$k_{concentrated} = \frac{3EI}{L^3} \; ; \; I = \frac{wt^3}{12} \tag{3a}$$

Equation (3a) denotes the equivalent spring constant of a concentrated load applied to a cantilever. For a uniform load model the equivalent spring constant becomes as below [16].

$$k_{uniform} = \frac{8EI}{L^3} \; ; \; I = \frac{wt^3}{12} \tag{3b}$$

2.2 Stability Analysis of a Wet Micro Cantilever

For the two kinds of forces mentioned in the previous section, one representing the amplitude of the mechanical restoring force and the other representing the capillary force can be plotted as a function of cantilever position z in Fig. 1(d). The mechanical restoring force F_{mech} changes linearly with the position z, and the capillary force F_{cap} changes with z in a nonlinear fashion as Eq. (4).

$$F_{cap} = \frac{2A\gamma_{la}\cos\theta_c}{z_0 - z} \tag{4}$$

Combine Eqs. (3) and (4), and reveal that there are multiple interception points for the two curves. The solution for the equilibrium position (or the identical deformation condition) is as below.

$$z^2 - z_0 z + \frac{2A\gamma_{la}\cos\theta_c}{k} = 0 \tag{5}$$

$$z = \frac{z_0}{2} \pm \sqrt{\left(\frac{z_0}{2}\right)^2 - \frac{2A\gamma_{la}\cos\theta_c}{k}} \tag{5a}$$

https://doi.org/10.1017/jmech.2015.50 Published online by Cambridge University Press

The graphical method can be used to illustrate the equilibrium position as the wetting area A changing. In Fig. 1(d) the equilibrium positions of the cantilever under several wetting area $A_1 \sim A_3$ can be found graphically. As the wetting area increases, the family of curves corresponding to the capillary force shifts upward.

At a particular wetting area, for example A_3 in Fig. 1(d), the two curves representing the mechanical restoring force and the capillary force intercept at one point Q tangentially. At this interception point Q, the tangent values of the two curves are also identical. The wetting area that involves such a condition can be defined as the "critical wetting area" or A_Q. So the identical slope condition is obtained as below.

$$z^2 - 2z_0 z + \left(z_0{}^2 - \frac{2A\gamma_{la}\cos\theta_c}{k} \right) = 0 \tag{6}$$

Combine Eqs. (5) and (6), give the deformation of the critical point Q.

$$z = \frac{z_0}{2} \tag{7}$$

This critical one-half gap deformation induced the surface tension for the unstable pull-down is believed to be found firstly in the literature. Meanwhile, substitute Eqs. (7) into (5) or (6), give the critical wetting area A_Q:

$$A_Q = \frac{k z_0{}^2}{8\gamma_{la}\cos\theta_c} \tag{8}$$

If the wetting area is further increased beyond A_Q in Eq. (8) or the induced deformation is beyond the one-half gap in Eq. (7), the two curves in Fig. 1(d) will not have a common interception. Thus the equilibrium point disappears. In fact, the capillary force will continue to increase while the mechanical restoring force, increasing linearly, is unable to catch up with the capillary force. The cantilever will be pulled downward to the bottom plate until touching for stiction.

Equation (7) states that the relative displacement of the cantilever beam from its rest position is one-half of the original spacing at the critical wetting area, Eq. (8). This one-half displacement is true irrespective of the actual spring constant. Compared to the static deformation of the full original spacing, the cantilever considering the stability issue in this work advances to stick with the relative displacement of one-half original spacing. In other words, the cantilever subject to capillary stiction herein is weaker than the one people have thought before.

The discussion of the relation between the length of residual liquid and critical gap is also helpful to the stiction phenomenon herein. The length of residual liquid x could be directly derived from the wetting area $A = xy$ in Eq. (8) as below.

$$x = \frac{k(z_0/2)^2}{2y\gamma_{la}\cos\theta_c} \tag{8a}$$

So the residual liquid x is proportional to the square of critical gap (z_0 / 2). It means that, the smaller the critical gap (z_0 / 2), the much smaller amount of the residual liquid. More specifically, if the critical gap is 10 times smaller, the residual liquid will be 100 times smaller (or almost no residual liquid). This phenomenon of almost no residual liquid also matches the capillary adhesion or stiction of a cantilever beam subjected to critical one-half gap mentioned in this paper.

In practice, Eq. (8) of the critical wetting area is more useful than the critical one-half gap position Eq. (7). The authors summarizes the capillary stiction parameters as well as the electrostatic pull-in and tries to conclude the similarity of them in Table 1. Additionally with the derivation sequence shown in the Appendix, the author obtained the generalized critical deformation (z_0 / N + 1) for any surface tension with the power law relationship to gap.

3. EXPERIMENT VERIFICATION

Some prior MEMS devices are verified again by the critical one-half gap criterion in this section.

3.1 Capillary Actuators for MAV Rudders

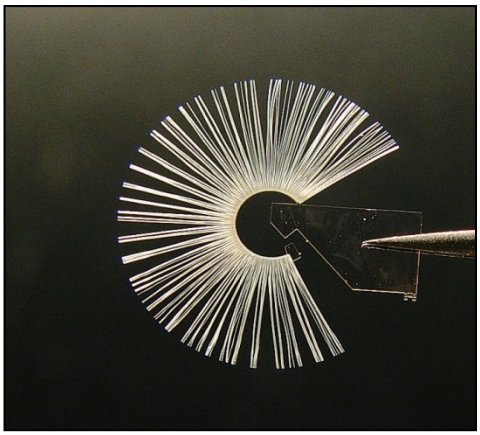
Peacock-like micro actuators that can generate obvious rotating strokes [11,12,17] and applied to the rudder of a micro-air-vehicle (MAV) were investigated to verify the fore mentioned theory of surface stiction. The device shown in Fig. 2 is made by SU-8 resist. A tweezer mounted in a steel housing with black backplate is used to grasp the SU-8 actuator device in the air firmly. Using water spray, the device is filled with water for capillary actuation right away and waits less than 1 min for water self-drying due to evaporation in ambient. With more than 200 comb-shaped cantilevers, the total actuation angles are around 224°. The device dimensions and material property are shown in the following.

$L = 2,700\mu\text{m}$ $E = 4.4\text{GPa}$
$w = 80\mu\text{m}$ $\gamma_{la} = 0.073\text{N/m}$
$t = 20\mu\text{m}$ $\theta = 70^0$
$z_0 = 20\mu\text{m}$

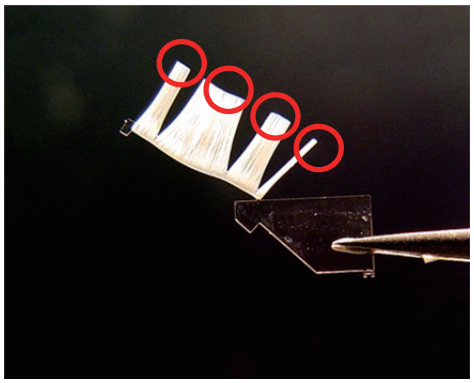
Table 1 Summary of surface forces and their critical gaps.

	Surface force	Critical gap	Check point
Capillary stiction ($N = 1$)	$\propto \frac{1}{(z_0 - z)}$	$\frac{z_0}{2}$	Critical wetting area
Electrostatic pull-in ($N = 2$)	$\propto \frac{1}{(z_0 - z)^2}$	$\frac{z_0}{3}$	Pull-in voltage
Generalized surface force with lower law relationship ($N > 0$)	$\propto \frac{1}{(z_0 - z)^N}$	$\frac{z_0}{N+1}$	Not yet well defined

https://doi.org/10.1017/jmech.2015.50 Published online by Cambridge University Press



(a) without water



(b) with water [11,12]

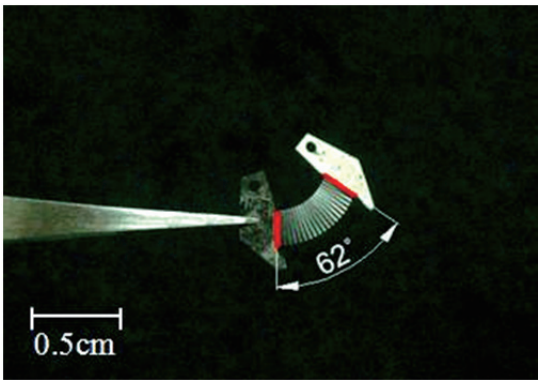
Fig. 2 Large angle change of the SU-8 actuator of 6 mm size.

Substituting the above parameters into Eq. (8) gives the critical wetting area as $A_Q / z_0^2 = 0.179$ or $A_Q = 71.6\mu m^2$. This critical area A_Q is much less than the maximum wetting area $Lw = 216,000\mu m^2$. It means that the cantilever beams are all stuck together after the consideration of stability. While the device wetted with water, several stuck places marked with circles in Fig. 2(b) are similar to the elasto-capillary result of Bico's work [18].

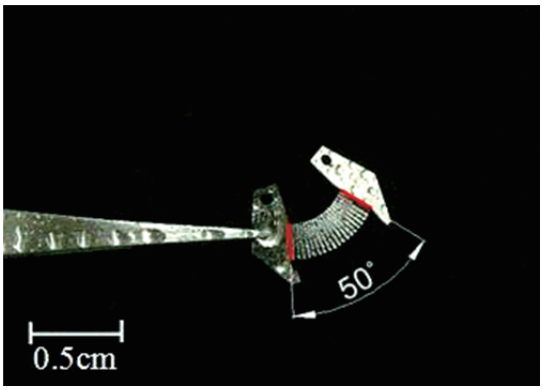
Moreover, as being changed with the structure material of SU-8 resist [12] to stainless steel (SUS-304) foil [17], the operations of this surface tension-driven actuator are depicted in Fig. 3. The dimension parameters and material property are shown as below.

$$L = 3,000\mu m \quad E = 200GPa$$
$$w = 40\mu m \quad \gamma_{la} = 0.073N/m$$
$$t = 50\mu m \quad \theta = 70^0$$
$$z_0 = 50\mu m$$

Substituting the above parameters into Eq. (8) gives the stiction area as $A_Q / z_0^2 = 46.36$ or $A_Q = 115,900\mu m^2$. Compared to the maximum wetting area $Lw = 120,000\mu m^2$, the critical wetting area A_Q is almost the same as wetting area Lw. In other words, if the contact angle is little bit larger than 70°, or the critical wetting area A_Q is less than Lw, then the stiction is no more. The actual rotation of the steel-based actuator (Fig. 3) is only 12° much less than the SU-8 case (Fig. 2) of 224°.



(a) steel actuator without water



(b) steel actuator with water [11,17]

Fig. 3 Small angle change of the parylene-coated steel bionic actuator due to the water surface tension.

3.2 Stiction of Parylene Beam-Actuators

In Ref. [19], some parylene cantilever beams have been fabricated to integrate an electrostatic micro-flap actuator. Their experimental results show that for 4.5μm thick parylene structures with 4.5μm thick sacrificial layer, no free-standing cantilever beams longer than 100μm can be made. For the different cantilever stiction models, referred to Refs. [6,7], a dimensionless peel number N_p [8,20] and the corresponding theoretical limit of detachment length $L_{critical} = L(N_p = 1)$ of cantilever beams are introduced as follows:

$$N_p = \frac{\text{restoring force}}{\text{adhesive force}} = \frac{3}{16}\frac{Et^3 z_0^{\,2}}{\gamma_{la}\cos\theta_c}\frac{1}{L^4} \tag{9}$$

$$L_{critical} = L(N_p = 1) = \sqrt[4]{\frac{3}{16}\frac{Et^3 z_0^{\,2}}{\gamma_{la}\cos\theta_c}} \tag{10}$$

Equation (10) can be also similarly derived from the critical wetting area Eq. (8) in this work. A stiffer cantilever with bigger Young's modulus E and beam thickness t can generate longer detachment length $L_{critical}$. Several models proposed by Mastrangelo [6], Tas [7] and this work are summarized in Table 2.

https://doi.org/10.1017/jmech.2015.50 Published online by Cambridge University Press

Table 2 Different models for detachment length of parylene cantilevers ($E = 4$GPa; $t = 4.5$μm; $z_0 = 4.5$μm; $\gamma_{la} = 0.073$N/m; $\theta_c = 75°$).

Model	N_p	$L_{critical}(N_p = 1)$ [μm]
Mastrangelo [6], Tas [7]	$\frac{3}{16}\frac{Et^3 z_0^2}{\gamma_{la}\cos\theta_c}\frac{1}{L^4}$	92.5 (stiffer cantilever)
Uniform load model of this work: Eqs. (3b) and (8)	$\frac{1}{12}\frac{Et^3 z_0^2}{\gamma_{la}\cos\theta_c}\frac{1}{L^4}$	75.5 (weaker cantilever)
Concentrated load model of this work: Eqs. (3a) and (8)	$\frac{1}{32}\frac{Et^3 z_0^2}{\gamma_{la}\cos\theta_c}\frac{1}{L^4}$	59.1 (much weaker cantilever)
Experiment data [19]	×	75 ~ 100

Referred to the experimental data in Ref. [19], Mastrangelo and Tas's model [6,7] is near to the upper limit, and the uniform load model in this work is near to the lower limit. It means that the mechanical behavior of cantilevers in this work considering the beam instability is softer than Mastrangelo and Tas's model which may take into account static equilibrium only. Adopting the elasto-capillary model of this work in designing the detachment length of cantilevers against capillary stiction is a more conservative and safer choice. In the future, other capillary actuators like the tap dance of a water droplet using electro-elasto-capillary (EEC) mechanism [21] could consider the critical one-half gap in this work.

4. CONCLUSIONS

In this note the authors theoretically found the critical one-half gap deformation for the pull down of a cantilever beam during its drying process by an elasto-capillary model. Extending this model with the generalized surface force of power law relationship to gap is also proposed. Some prior MEMS devices including MAV rudder and parylene beam actuator are demonstrated as examples to verify this critical one-half gap deformation model.

ACKNOWLEDGEMENTS

The authors appreciate the financial support from the Ministry Of Science and Technology (MOST) of Taiwan with the research project numbers of 101-2623-E-032-001-MY3 and 103-2221-E-032-034.

APPENDIX

Derivation of the Critical Gap for the Generalized Surface Force with Power Law To Gap

Herein the author generalized the surface force $F_{surface}$ with power law to gap as Eq. (A1). The power-law coefficient α has not yet been defined. The pull back force F_{mech} in Eq. (A2) for a cantilever is the same as Eq. (3).

$$F_{surface} = \frac{\alpha}{(z_0 - z)^N} \tag{A1}$$

$$F_{mech} = kz \tag{A2}$$

For satisfying the force balance (or identical deformation condition), equalize Eqs. (A1) and (A2) and give Eq. (A3).

$$z(z_0 - z)^N - \frac{\alpha}{k} = 0 \tag{A3}$$

For satisfying the identical slope condition, firstly take the 1st derivative of Eqs. (A1) and (A2), with respect to z.

$$F_{surface}' = \frac{N\alpha}{(z_0 - z)^{N+1}} \tag{A4}$$

$$F_{mech}' = k \tag{A5}$$

Equalize Eqs. (A4) and (A5) and give Eq. (A6).

$$\frac{1}{N}(z_0 - z)^{N+1} - \frac{\alpha}{k} = 0 \tag{A6}$$

Finally combine Eqs. (A3) and (A6), eliminate the term (α/k), and find the generalized critical deformation as Eq. (A7).

$$z = \frac{z_0}{N+1} \tag{A7}$$

The corresponding check point corresponding to the generalized critical deformation in Table 1 is not yet defined and waits for the physical interpretation of coefficient α.

REFERENCES

1. de Genes, P. G., "Wetting: Statics and Dynamics," *Reviews of Modern Physics,* **57**, pp. 827–890 (1985).
2. Israelachvili, J. N., *Intermolecular and Surface Forces*, Academic Press, UK, p. 120 (1985).
3. Madou, M., *Fundamentals of Microfabrication*, 1st Edition, CRC Press, New York, USA, p. 433 (1997).
4. Mastrangelo, C. H. and Hsu, C. H., "A Simple Experimental Technique for the Measurement of the Work of Adhesion of Microstructures," *Proceedings of IEEE Solid-State Sensors and Actuators Workshop*, Hilton Head Island, SC, USA, pp. 208–212 (1992).
5. Mastrangelo, C. H. and Hsu, C. H., "Mechanical Stability and Adhesion of Microstructures under Capillary Forces - Part I: Basic Theory," *Journal of Microelectromechanical Systems*, **2**, pp. 33–43

https://doi.org/10.1017/jmech.2015.50 Published online by Cambridge University Press

(1993).
6. Mastrangelo, C. H. and Hsu, C. H., "Mechanical Stability and Adhesion of Microstructures under Capillary Forces — Part II: Experiments," *Journal of Microelectromechanical Systems*, **2**, pp.44–55 (1993).
7. Tas, N., Sonnenberg, T., Jansen, H., Legtenberg, R. and Elwenspoek, M., "Stiction in Surface Micromachining," *Journal of Micromechanics and Microengineering*, **6**, pp. 385–397 (1996).
8. Zhao, Y. P., Wang, L. S. and Yu, T. X., "Mechanics of Adhesion in MEMS - A Review," *Journal of Adhesion Science and Technology*, **17**, pp. 519–546 (2003).
9. Wei, Z. and Zhao, Y. P., "Growth of Liquid Bridge in AFM," *Journal of Physics D: Applied Physics*, **40**, pp. 4368–4375 (2007).
10. Yang, L. J., Yao, T. J. and Tai, Y. C., "The Marching Velocity of the Capillary Meniscus in a Microchannel," *Journal of Micromechanics and Microengineering*, **14**, pp. 220–225 (2004).
11. Yang, L. J., Liu, K. C. and Lin, W. C., "On Deriving Surface Tension Forces in MEMS," *Journal of Applied Science and Engineering*, **17**, pp. 223–230 (2014).
12. Yang, L. J. and Liu, K. C., "Surface Tension-Driven Micro Valves with Large Rotating Stroke," *Tamkang Journal of Science and Engineering*, **10**, pp. 141–146 (2007).
13. Loke, Y., McKinnon, G. H. and Brette, M. J., "Fabrication and Characterization of Silicon Micromachined Threshold Accelerometers," *Sensors and Actuators A: Physical*, **29**, pp. 235–240 (1991).
14. Degani, O., "Pull-in Study of an Electrostatic Torsion Mirror," *Journal of Microelectromechanical Systems*, **7**, pp. 373–379 (1998).
15. Wang, H. J., "Capillary of Rectangular Micro Grooves and Their Applications to Heat Pipes," *Tamkang Journal of Science and Engineering*, **8**, pp. 249–255 (2005).
16. Gere, G. M. and Timoshenko, S. P., *Mechanics of Materials*, 2nd Edition, Wadsworth Publishing Co. Inc., Belmont, CA, USA, pp. 736–737 (1984).
17. Yang, L. J., Jan, D. L. and Lin, W. C., "Steel-Based Bionic Actuators for Flapping Micro-air-vehicles," *Micro and Nano Letters*, **8**, pp. 686–690 (2013).
18. Bico, J., Roman, B., Moulin, L. and Boudaoud, A., "Elastocapillary Coalescence in Wet Hair," *Nature*, **432**, p. 690 (2004).
19. Yao, T. J., Yang, X. and Tai, Y. C., "BrF_3 Dry Release Technology for Large Freestanding Parylene Microstructures and Electrostatic Actuators," *Sensors and Actuators A: Physical*, **97-98**, pp. 771–775 (2002).
20. van Spengen, W. M., Puers, R. and De Wolf, I., "The Prediction of Stiction Failure in MEMS," *IEEE Transactions on Device and Materials Reliability*, **3**, pp. 167–172 (2003).
21. Wang, Z., Wang, F. C. and Zhao, Y. P., "Tap Dance of a Water Droplet," *Proceedings of the Royal Society A*, **468**, pp. 2485–2495 (2012).

(Manuscript received November 21, 2014,
accepted for publication March 27, 2015.)

https://doi.org/10.1017/jmech.2015.50 Published online by Cambridge University Press